

# Influence of Growth Phase on Bacterial Deposition: Interaction Mechanisms in Packed-Bed Column and Radial Stagnation Point Flow Systems<sup>†</sup>

SHARON L. WALKER,<sup>\*,‡</sup>  
JEREMY A. REDMAN,<sup>§</sup> AND  
MENACHEM ELIMELECH<sup>||</sup>

Department of Chemical and Environmental Engineering,  
University of California, Riverside, Riverside, California 92521,  
Department of Civil Engineering and Construction  
Engineering Management, California State University, Long  
Beach, California 90840-8306, and Department of Chemical  
Engineering, Environmental Engineering Program, Yale  
University, New Haven, Connecticut 06520-8286

The influence of bacterial growth stage on cell deposition kinetics has been examined using a mutant of *Escherichia coli* K12. Two experimental techniques—a packed-bed column and a radial stagnation point flow (RSPF) system—were employed to determine bacterial deposition rates onto quartz surfaces over a wide range of solution ionic strengths. Stationary-phase cells were found to be more adhesive than mid-exponential phase cells in both experimental systems. The divergence in deposition behavior was notably more pronounced in the RSPF than in the packed-bed system. For instance, in the RSPF system, the deposition rate of the stationary-phase cells at 0.03 M ionic strength was 14 times greater than that of the mid-exponential cells. The divergence in the packed-bed system was most significant at 0.01 M, where the deposition rate for the stationary-phase cells was nearly 4 times greater than for the mid-exponential cells. To explain the observed adhesion behavior, the stationary and mid-exponential bacterial cells were characterized for their size, surface charge density, electrophoretic mobility, viability, and hydrophobicity. On the basis of this analysis, it is suggested that the stationary cells have a more heterogeneous distribution of charged functional groups on the bacterial surface than the mid-exponential cells, which results in higher deposition kinetics. Furthermore, because the RSPF system enumerates only bacterial cells retained in primary minima, whereas the packed column captures mostly cells deposited in secondary minima, the difference in the stationary and mid-exponential cell deposition kinetics is much more pronounced in the RSPF system.

## Introduction

Understanding the factors influencing bacterial deposition and transport is important for a number of environmental

processes, such as in situ bioremediation (1) and filtration of microorganisms in porous media (2). By studying microbial adhesion mechanisms, we also gain insight into processes such as the initiation of infection (3–5), biofilm formation (6, 7), and the colonization of plant roots (8, 9). The physical and chemical factors governing bacterial adhesion in aquatic systems—such as cell type (10, 11), hydrophobic interactions (11–13), motility (14, 15), surface charge characteristics (13, 16), and surface macromolecules (lipopolysaccharides, fimbriae) (17–20)—have been studied extensively. However, the mechanisms governing the adhesion of bacterial cells onto mineral surfaces are not yet fully understood, in large part because of wide variation in the choice of experimental protocols and techniques.

Previously, bacterial deposition under flow conditions has been studied in several systems, including packed columns (17, 21–23), parallel-plate flow chambers (24–26), and radial stagnation point flow cells (23, 27, 28). The hydrodynamic conditions and type of interaction mechanisms captured in each apparatus differ (23, 27), such that results between systems are not necessarily comparable. Another source of variability in these adhesion studies has been the growth phase of cells utilized (9, 24, 28). Often overlooked is the fact bacteria are living organisms that exhibit metabolic and physiological changes (29), likely affecting their adhesive properties (24, 30).

It has been established that the predominant functional groups exposed on the outer membrane of *E. coli* are amino and carboxyl groups on membrane proteins and phosphate and carboxyl groups on both lipopolysaccharide (LPS) and extracellular polymeric substances (EPS)-associated carbohydrates (31–33). The extent of protein coverage (29, 34), EPS coverage (35), and LPS conformation (29, 32) evolve as a function of growth phase and, thus, likely contribute to the chemical heterogeneity of the bacterial surface. Theoretical and experimental studies have demonstrated that the presence of surface charge heterogeneity can decrease electrostatic repulsion at the local scale and increase the rate of irreversible particle attachment (36–41). Therefore, how increasing culture age influences the extent of cell surface charge heterogeneity and subsequently the deposition kinetics must be addressed.

The objective of this paper is to examine the influence of growth phase on the initial stage of bacterial deposition under well-controlled solution chemistry and hydrodynamic conditions. Deposition experiments were conducted using cells harvested at mid-exponential and stationary growth phase. Two experimental techniques—a packed-bed column and a radial stagnation point flow (RSPF) system—were used because they enable the evaluation of differing combinations of deposition mechanisms. Cell characterization techniques were further employed to delineate the extent to which growth phase alters cell surface heterogeneity and how this ultimately affects deposition kinetics in the packed-bed column and RSPF systems.

## Materials and Methods

**Bacterial Cell Preparation and Growth.** *Escherichia coli* K12 D21, used in this study, was obtained from the *E. coli* Genetic Stock Center at Yale University. The *E. coli* D21 mutant was selected because the LPS and outer membrane have previously been characterized (28, 31, 42). It has been reported as nonmotile (43), lacking the O-antigen (28), and producing little or no EPS (44). To visualize the cells in the adhesion studies, a plasmid coding for an enhanced green fluorescing protein and gentamicin resistance (45) was introduced to

<sup>†</sup> This paper is part of the Charles O'Melia tribute issue.

\* Corresponding author phone: (951)827-6094; fax: (951)827-5696; e-mail: swalker@engr.ucr.edu.

<sup>‡</sup> University of California, Riverside.

<sup>§</sup> California State University.

<sup>||</sup> Yale University.

the native D21 cell by electroporation (46). The resulting transformed D21 cell line is referred to as D21g.

Cells were grown in Luria-Bertani broth (LB Broth, Fisher Scientific, Fair Lawn, NJ) supplemented with 0.03 mg/L gentamicin (Sigma, St. Louis, MO) at 37 °C until reaching the desired growth stage (3 and 18 h corresponding to mid-exponential and stationary phases), at which time they were harvested for use. The cells were pelleted by centrifugation (Sorvall RC26 Plus Centrifuge) for 15 min at 3823g via a SS34 rotor (Kendro Laboratory Products, Newtown, CT). The growth medium was decanted, and the pellet was resuspended in a KCl electrolyte solution (0.01 M). The cells were pelleted and rinsed with fresh electrolyte solution in this manner two additional times to remove traces of the growth medium (23, 47).

**Bacterial Characterization.** The electrophoretic mobility of the bacterial cells was determined by diluting the rinsed cell pellet in a KCl electrolyte solution at a final concentration of  $10^5$ – $10^6$  cells/mL. Electrolyte solutions were prepared with deionized water (Barnstead Thermolyne Corporation, Dubuque, IA) and reagent-grade KCl (Fisher Scientific) at ambient pH (5.6–5.8). Electrophoretic mobility measurements were conducted at 25 °C using a ZetaPALS analyzer (Brookhaven Instruments Corporation, Holtsville, NY) and were repeated a minimum of three times at each ionic strength using freshly rinsed cells. Electrophoretic mobilities were converted to  $\zeta$ -potentials using the tabulated numerical calculations of Ottewill and Shaw, which account for retardation and relaxation effects (48).

An inverted fluorescent microscope (Axiovert 200m, Zeiss, Thornwood, NY) operating in phase contrast mode was used to take images of D21g cells harvested after 3 and 18 h of growth after resuspension in an electrolyte solution (ca.  $10^7$  cells/mL in 0.01 M KCl). The images were imported into an image processing program (ImageJ, NIH) and analyzed using the built-in particle analysis routines. From the measured cell lengths and widths, the average equivalent spherical radii of the D21g cells were determined.

Viability tests were performed using the Live/Dead BacLight kit (L-7012, Molecular Probes, Eugene, OR). An inverted fluorescent microscope (Zeiss, Thornwood, NY), operating in fluorescent mode, allowed for the enumeration of viable D21g cells under the solution conditions of the adhesion experiments and cell characterization techniques.

The hydrophobicity of the mid-exponential and stationary-phase cells was measured using the microbial adhesion to hydrocarbons (MATH) test (47) with *n*-dodecane (laboratory grade, Fisher Scientific). Samples were prepared by transferring 4 mL of a cell solution (optical density of 0.20–0.25 in 0.01 M KCl at 546 nm) to a test tube containing 1 mL of dodecane. Test tubes were vortexed (Touch Mixer model 231, Fisher Scientific) for 2 min followed by a 15 min rest period to allow for phase separation. The optical density of the cells in the aqueous phase was measured at 546 nm (Hewlett-Packard model 8453) to determine the extent of bacterial cell partitioning between the dodecane and the electrolyte. Hydrophobicity is reported as the percent of total cells partitioned into the hydrocarbon (47).

Potentiometric titration of mid-exponential and stationary-phase cells was conducted to determine the relative acidity of the bacterial surfaces using a microtitrator (794 Basic Titrino, Metrohm, Switzerland). Prior to titration, the solution pH was lowered to 4 by addition of HCl, and the solution was purged with N<sub>2</sub> gas to remove any dissolved carbon dioxide present. Titrations were performed on solutions of bacteria suspended in 0.01 M KCl (concentration between  $10^8$  and  $10^{10}$  cells/mL). Acidity and the corresponding surface charge density were determined from the amount of NaOH consumed during a titration between pH 4 and pH 10 (49). The surface charge density, calculated from the acidity

and accounting for the surface area of a cell, provides a measure of the total charged functional groups on the outer membrane surface.

**Packed-Bed Column Deposition Experiments.** Bacterial transport experiments were conducted in glass chromatography columns packed with clean quartz grains. Sieve analysis resulted in an average grain diameter ( $d_{50}$ ) of 205  $\mu$ m and a coefficient of uniformity ( $d_{60}/d_{10}$ ) of 1.26. The cleaning procedure and size analysis for the quartz sand have been reported previously (23, 28). An adjustable bed height column (Omnifit USA, Toms River, NJ) with a 1-cm i.d. was packed to a porosity of 0.43, as determined gravimetrically. The ionic strength of the pore fluid ranged from 0.001 to 0.1 M KCl. All solutions had an ambient pH between 5.6 and 5.8 at room temperature (22–25 °C). The approach (superficial) velocity during the column experiments was 0.021 cm/s. A more extensive description of methods employed for wet-packing, column equilibration, and transport experiments has been given in our recent studies (23, 28).

To quantitatively compare the deposition (adhesion) kinetics of the *E. coli* cells harvested at mid-exponential and stationary growth phase, and at the different solution ionic strengths, the deposition rate coefficient ( $k_d$ ) was determined using (50)

$$k_d = -\frac{U}{fL} \ln\left(\frac{C}{C_0}\right) \quad (1)$$

Here,  $C/C_0$  is the normalized breakthrough concentration relevant to "clean bed" conditions,  $U$  is the approach (superficial) fluid velocity,  $f$  is the packed-bed porosity, and  $L$  is the length of the packed-bed. The clean bed  $C/C_0$  was determined for each experiment by averaging the normalized breakthrough concentrations measured between 1.8 and 2 pore volumes.

For transport experiments under favorable (non-repulsive) electrostatic conditions, the quartz was silanized by suspension in a 1% solution of 3-aminopropyl-triethoxysilane (Sigma) for 5 min, followed by thorough rinsing in deionized water and curing at 80 °C for 24 h (23, 28). Under these conditions a favorable deposition rate ( $k_{d, fav}$ ) was determined.

**Radial Stagnation Point Flow System.** Bacterial deposition experiments were also conducted in a radial stagnation point flow (RSPF) system following the protocol developed in our earlier studies (23, 28). A flow rate of 5 mL/min, corresponding to a particle Peclet number (51) of 2.4, was selected to be comparable to the particle Peclet number estimated for the packed column. Round quartz cover slips with a 25 mm diameter and 0.1 mm thickness (Electron Microscopy Sciences, Ft. Washington, PA) were cleaned and prepared for use in the RSPF flow cell as described elsewhere (23, 28).

Bacterial deposition onto the quartz surface in the radial stagnation point flow system is presented as a transfer rate coefficient ( $k_{RSPF}$ ). It is related to the bacterial deposition flux (number of cells per area per time;  $J$ ) and the bulk bacterial concentration ( $C_0$ ) via

$$J = k_{RSPF} C_0 \quad (2)$$

The cell deposition flux was determined by normalizing the initial slope of the number of deposited particles versus time curve by the microscope viewing area (210  $\mu$ m  $\times$  165  $\mu$ m).

For adhesion experiments under favorable (non-repulsive) electrostatic conditions, the slides were chemically modified with aminosilane. One side of the quartz cover slip was exposed to a 0.2% (vol/vol) mixture of (aminoethylaminomethyl)-phenethyltrimethoxysilane (Gelest, Inc. Tullytown, PA) in ethanol for 3–5 min at room temperature and then cured for 90 min at 130 °C (23, 28). The slide was then rinsed with

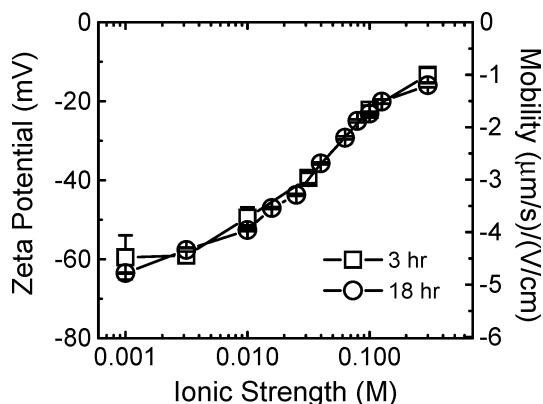


**FIGURE 1.** Electrophoretic mobility and  $\zeta$ -potential of *E. coli* D21g cells harvested at 3 and 18 h (corresponding to mid-exponential and stationary growth phase cells) as a function of ionic strength (KCl). Error bars indicate one standard deviation.

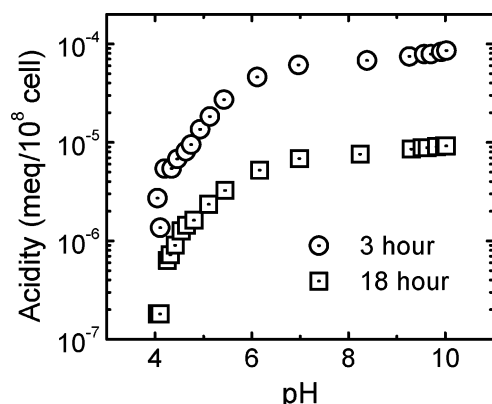


**FIGURE 2.** Potentiometric titration of mid-exponential and stationary-phase *E. coli* D21g cells. Acidity is presented as meq per  $10^8$  bacterial cells determined from the amount of NaOH consumed at each interval between pH 4 and pH 10 in  $10^{-2}$  M KCl and temperature of 25 °C.

DI water and installed in the radial stagnation point flow cell. Under these conditions, a favorable transfer rate coefficient ( $k_{RSPF, fav}$ ) can be determined by the relationship expressed in eq 2. Note that although the aminosilane used to modify the quartz cover slip is different than that used for the quartz grains, both aminosilane molecules yield positively charged collector surfaces, resulting in favorable deposition conditions.

## Results and Discussion

**Bacterial Cell Characteristics.** The measured electrophoretic mobilities and corresponding calculated  $\zeta$ -potentials (Figure 1) indicate that the bacterial cells are negatively charged under all the conditions of the experiments. Under the solution conditions analyzed, the quartz surfaces are also negatively

charged (23, 28), implying repulsive electrostatic interactions will dominate between cells and quartz in either experimental system. A notable observation in Figure 1 is the indistinguishable  $\zeta$ -potentials for the mid-exponential and stationary-phase cells.

Potentiometric titration was used to evaluate the density of charge on the cell surface. Results of the cell titrations are presented in Figure 2. Acidity, or titrated charge, relates to the amount of base required to neutralize the cell surface dissociable groups at each pH increment between pH 4 and pH 10. The shapes of the titration curves for the 3 and 18 h cells are comparable, suggesting that the types of functional groups are unchanging with growth phase, even if the density of the charged groups is not. From the total amount of base consumed during titration, total acidity and the corresponding surface charge density were calculated. The total acidity values for mid-exponential and stationary-phase cells were  $7.1 \times 10^{-5}$  and  $8.4 \times 10^{-6}$  meq/ $10^8$  cell, respectively. The corresponding surface charge densities were determined to be  $796.8 \mu\text{C}/\text{cm}^2$  for the 3 h cells and  $87.9 \mu\text{C}/\text{cm}^2$  for the 18 h cells. The titration experiments point out that mid-exponential cells are substantially more acidic than stationary-phase cells. The surface charge value for 3 h cells indicates a much higher number of dissociable functional groups and greater charge density existing on the bacterial surface as compared to the 18 h cells. These results are presented in Table 1 along with other parameters that will be discussed later.

Bacterial cell size was determined for cells harvested at mid-exponential and stationary growth phases. Using the experimentally measured lengths and widths of cells—3.7 and 1.2  $\mu\text{m}$  for the 3 h cells and 3.6 and 1.3  $\mu\text{m}$  for the 18 h cells—the equivalent spherical radius was calculated. The equivalent radii for the 3 and 18 h cells were determined to be very similar at 0.87 and 0.93  $\mu\text{m}$ , respectively,

Further characterization of the cells using the Live/Dead BacLight kit found the extent of viable mid-exponential and stationary-phase cells in suspension was identical. Specifically, the viability in salt solutions ranging from 0.01 to 0.3 M KCl averaged 79% and 80% for the 3 and 18 h cell cultures, respectively.

The final characterization tool performed on the mid-exponential and stationary-phase cells was the measurement of hydrophobicity by the microbial adhesion to hydrocarbon (MATH) test. Hydrophobicity was found to change with growth phase (Table 1), namely, 16% of the 3 h cells partitioned into dodecane, whereas 34% of the 18 h cells partitioned into the hydrocarbon.

**Bacterial Deposition Kinetics in Packed-Bed.** As can be seen in Figure 3, cell deposition rates ( $k_d$ ) were governed by solution ionic strength. Deposition rates increased by more than 2 orders of magnitude over the range of salt concentrations examined for cells harvested at both mid-exponential and stationary phases. At intermediate ionic strengths, the

**TABLE 1.** Characterization of *E. coli* D21g Cells as a Function of Growth Stage

growth stage	growth time (h)	% live <sup>a</sup>	cell radius ( $\mu\text{m}$ ) <sup>b</sup>	MATH (%) <sup>c</sup>	$k_{d, fav}$ ( $\text{s}^{-1}$ )	$k_{RSPF, fav}$ (m/s)	acidity (meq/ $10^8$ cell) <sup>d</sup>	charge density ( $\mu\text{C}/\text{cm}^2$ ) <sup>e</sup>
mid-exponential	3	83 ± 5	0.87	16 ± 1	$3.35 \times 10^{-2}$	$2.5 \times 10^{-7}$	$7.1 \times 10^{-5}$	796.8
stationary	18	81 ± 2	0.93	34 ± 6	$3.49 \times 10^{-2}$	$2.6 \times 10^{-7}$	$8.4 \times 10^{-6}$	87.9

<sup>a</sup> Percentage of viable cell population determined by the Live/Dead BacLight kit. Values are an average for cells evaluated in 10 mM KCl. <sup>b</sup> Value for equivalent spherical radius calculated from experimentally measured length and width of individual cells. The average lengths and widths of the cells were 3.7 and 1.2  $\mu\text{m}$  for the 3 h cells and 3.6 and 1.3  $\mu\text{m}$  for the 18 h cells, respectively. <sup>c</sup> Microbial adhesion to hydrocarbons (MATH) indicates the relative hydrophobicity of the cell as the percent of cells partitioned in dodecane versus electrolyte (10 mM KCl). <sup>d</sup> Acidity determined from the amount of NaOH consumed during a titration between pH 4 and pH 10 for cells suspended in 10 mM KCl. <sup>e</sup> Surface charge density indicates the density of charged functional groups across the cell surface. Value determined from the experimentally measured acidity, accounting for the exposed surface area of the cells (calculated for a spherical cell) and Faraday's constant of 96 485 C/mol.

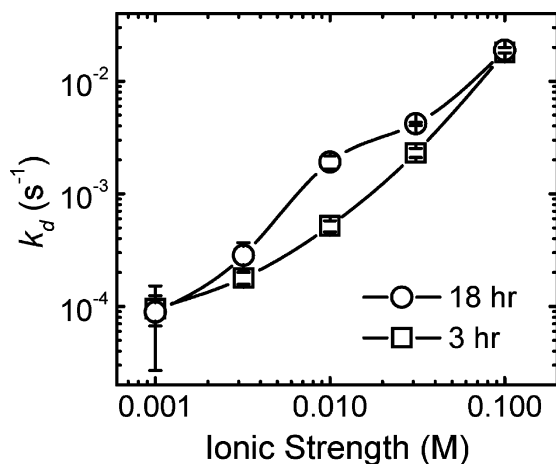


**FIGURE 3.** Bacterial deposition rate ( $k_d$ ) as a function of ionic strength within the packed-bed column for *E. coli* D21g cells harvested at mid-exponential and stationary phases (3 and 18 h, respectively). Experimental conditions were as follows: approach velocity = 0.021 cm/s, porosity = 0.43, mean grain diameter = 205  $\mu\text{m}$ , temperature = 22–25  $^{\circ}\text{C}$ , and pH = 5.6–5.8. Error bars indicate one standard deviation.

18 h cells were consistently more adhesive than their 3 h counterparts. The observed trends in the deposition rate within the packed-bed are consistent with the  $\zeta$ -potential behavior (Figure 1), reflecting the paramount role of electrostatic double layer repulsion in cell adhesion.

To gain further insight into the interaction forces governing D21g cell deposition, the classic Derjaguin–Landau–Verwey–Overbeek (DLVO) theory (52) has been applied to calculate the total interaction energy as a function of separation distance between the bacterium and quartz surface (23). In these calculations, the  $\zeta$ -potentials (Figure 2) are used instead of surface potentials and a Hamaker constant of  $6.5 \times 10^{-21}$  J is used for the bacterium–water–quartz system (23, 28). Because the cell size and  $\zeta$ -potentials for the 3 and 18 h cells are nearly identical, the DLVO calculations predict similar interaction energy profiles for both stationary and mid-exponential cells. Surprisingly, however, deposition rates of 3 and 18 h cells are quite different at intermediate ionic strengths (Figure 3), suggesting an underlying difference between cells with culture age. The possible differences between the mid-exponential and stationary-phase cells contributing to the adhesion behavior will be discussed further in a following section.

**Bacterial Deposition Kinetics in the RSPF System.** The deposition kinetics of the 3 and 18 h cells as a function of ionic strength are presented in Figure 4. Stationary-phase cells were substantially more adhesive than mid-exponential phase cells across the entire range of solution ionic strengths examined. Cell deposition was governed by ionic strength, with higher ionic strengths resulting in greater  $k_{\text{RSPF}}$  values. Other than this general trend, the deposition behavior for 3 and 18 h cells differed significantly in the RSPF system. Specifically, the  $k_{\text{RSPF}}$  for 18 h cells reaches a plateau between 0.1 and 0.3 M KCl, whereas 3 h cells had not yet reached a plateau at the highest ionic strength condition tested. However, at 0.3 M the bacterial transfer rates are the same for both 3 and 18 h cells. This indicates entrance into the mass-transfer-limited regime, where a further increase in ionic strength will not affect the deposition rate. Another variation in the deposition behavior occurred at 0.03 M, below which deposition of 3 h cells was statistically insignificant, even when the bulk cell concentration was increased to  $10^8$  cell/mL. This further supports our conclusion regarding the much lower adhesive characteristic of the mid-exponential phase cells as compared to the stationary-phase cells.

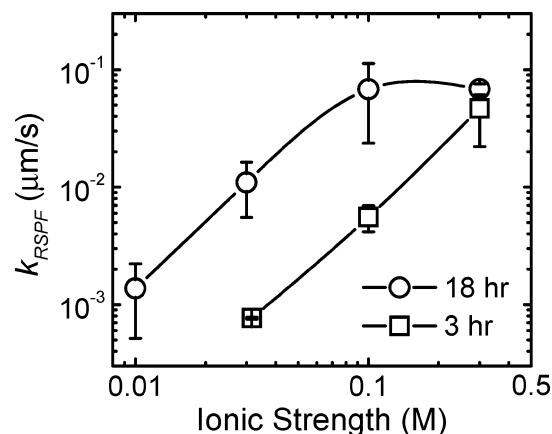


**FIGURE 4.** Variation of bacterial transfer rate coefficient ( $k_{\text{RSPF}}$ ) with ionic strength for the RSPF system. *E. coli* cells were harvested at mid-exponential and stationary phases (3 and 18 h, respectively). Experimental conditions were as follows: RSPF capillary flow velocity = 0.0265 m/s, temperature = 22–25  $^{\circ}\text{C}$ , and pH = 5.6–5.8. Error bars indicate one standard deviation.

**Possible Causes for the Difference in Adhesion between Mid-exponential and Stationary-Phase Cells.** Bacterial deposition is controlled by two major factors: the transport to a collector surface and the subsequent interactions between bacterial cell and collector surface that arise on close approach. The size of the cell and the hydrodynamics of the system control transport of the bacteria, while the attachment is determined by the near-surface interactions, such as DLVO-type forces. The bulk parameters that affect transport and DLVO interactions are nearly identical for cells harvested at different growth phases, yet deposition kinetics are markedly different. Not only is the deposition rate of 18 h cells higher than the 3 h cells, but also the deposition kinetics are strikingly different in the packed-bed and RSPF systems. These observations suggest an underlying distinction between cells of different culture age that can be attributed to subtle, local-scale cell characteristics often overlooked in transport studies. Such characteristics that may explain the adhesive nature of the D21g cells include electrokinetic properties, cell viability, cell size, EPS production, surface charge, and cell hydrophobicity. Each will be discussed in the following subsections.

**(a) Electrokinetic Properties.** The  $\zeta$ -potential values were determined to be virtually identical for the mid-exponential and stationary-phase cells (Figure 1). Thus, the deposition behavior in Figures 3 and 4 cannot be explained by conventional electrostatic interactions alone. The  $\zeta$ -potential is a measure of the electrical potential existing at the electrokinetic shear plane. The shear plane is located in close proximity to the outer membrane surface, although its exact location cannot be predicted for “soft” bacterial cells due to the presence of surface macromolecules (26). The  $\zeta$ -potential is a *macroscopic* parameter that reflects the *net* or average electrokinetic properties of the cell and is not sensitive to small local-scale variations on the cell surface. Therefore, this parameter does not capture the subtle differences in charge heterogeneity on the surface and LPS of mid-exponential and stationary-phase cells. As we discuss later, local surface charge heterogeneities on bacterial cells can have a marked effect on cell adhesion.

**(b) Cell Viability.** An equal percentage of cells were viable when harvested at mid-exponential and stationary phases, as indicated in Table 1. If the cell viability varied with culture age, the observed adhesive behavior could be attributed to the fraction of viable cells in solution; however, this is not the case. Therefore, this parameter does not explain the differences in the observed deposition kinetics.

**(c) Cell Size.** It was observed that stationary-phase cells were slightly shorter and wider with a measured length and width at 3.6 and 1.3  $\mu\text{m}$ , respectively. The mid-exponential phase cells had a length of 3.7  $\mu\text{m}$  and a width of 1.2  $\mu\text{m}$ . These data agree with the previously reported observation that *E. coli* becomes somewhat smaller and less rod-shaped in stationary phase (53). This subtle difference in size may influence transport of the bacteria to the quartz surface. To establish whether the minor difference in cell size with growth phase alters the cell transfer rate, experiments were carried out under favorable (non-repulsive) conditions in the RSPF system with positively charged, aminosilane-modified quartz slides. The subsequent interaction between oppositely charged surfaces allows for the determination of  $k_{\text{RSPF}}$  under mass-transport-limited conditions (referred to as  $k_{\text{RSPF, fav}}$ ). As reported in Table 1, this favorable deposition scenario produced virtually identical bacterial transfer rates ( $k_{\text{RSPF, fav}}$ ) of  $2.5 \times 10^{-7}$  and  $2.6 \times 10^{-7}$  m/s for 3 and 18 h cells, respectively. These results confirmed that the difference between 3 and 18 h cell deposition behavior is not size related.

**(d) EPS Production.** Bacterial adhesion and the strengthening of attachment has been attributed to the presence of EPS (9, 54). EPS has also been credited with contributing to the overall heterogeneous nature of bacterial surfaces (54–56). The *E. coli* D21 mutant selected for this study has been reported as producing a negligible amount of EPS (44); therefore, we do not attribute the deposition trends or the heterogeneous nature of the cells to EPS.

**(e) Surface Charge.** Potentiometric titration allows for evaluation of the extent of charged functional groups on the cell surface. Mid-exponential phase cell surfaces have a greater number of dissociable groups and a higher charge density than the stationary-phase cells, as indicated by the higher value of surface charge and acidity (Table 1). These results are attributed in part to the presence of outer membrane proteins, which are more abundant on the surface of mid-exponential phase cells (29); however, some acidity is credited to the presence of dissociable groups exposed on the LPS. The density and distribution of charge existing on the bacteria influence the degree of electrostatic repulsion occurring between the cell and collector surface, which, in turn, impacts the rate of irreversible attachment in the primary minimum. The experiments with mid-exponential phase cells, having higher surface charge density, resulted in lower bacterial transfer rate coefficients (Figure 4) and deposition rates (Figure 3) than the stationary-phase cells, presumably due to greater electrostatic repulsion. This phenomenon will be discussed in greater detail in the final section of the paper.

**(f) Cell Hydrophobicity.** Relative cell hydrophobicity can provide insights into the evolving types of chemical species on bacterial surfaces. A greater amount of polar and acidic molecules exposed on the surface of the cells would result in a lower percentage of cells partitioning into the hydrocarbon. The MATH test data (Table 1) may suggest that outer membrane proteins of *E. coli* are mostly hydrophilic (acidic) and decrease in number with culture age (29, 33), yielding a corresponding increase in hydrophobicity. Further evidence of the sensitivity of bacterial hydrophobicity to the protein presence can be found in the literature (24, 57, 58). As we discuss below, the larger number of exposed polar molecules, due to the greater abundance of proteins present on mid-exponential phase cells, contribute to a more uniform distribution of chemical functional groups and charge on the bacterial surface. The local distribution of polar functional groups, in turn, impacts the extent of electrostatic interactions and, subsequently, the kinetics of bacterial deposition on the collector surface.

**Growth Phase Influences Cell Charge Heterogeneity and Deposition Kinetics.** The variation in deposition kinetics for

mid-exponential and stationary-phase cells is explained by considering the evolution in local-scale surface charge heterogeneity with culture age. At the pH of our experiments (5.6–5.8), the dominant ionic species exposed on the outer membrane of the *E. coli* D21g arise from negatively charged phosphate groups associated with the LPS (33, 59) and carboxyl groups associated with both proteins and polysaccharides (59). The origin of the ionic species does not vary with growth phase, as confirmed by the similar shapes of the titration curves in Figure 2. Therefore, the adhesive behavior of the cells is not attributed to the type of ionic species but to the distribution (or homogeneity) of functional groups exposed on cellular structures. Our characterization techniques support this assertion. Both the titration and MATH test results suggest that mid-exponential phase cells have a higher charge density and larger amount of polar molecules exposed, due to greater abundance of proteins on mid-exponential phase cells than on stationary-phase cells. Consequently, upon approach toward the collector surface, the mid-exponential phase cells will appear more uniformly charged. In contrast, stationary-phase cells—with fewer exposed proteins and a greater number of phosphate groups on the LPS (29, 32)—will have a more heterogeneous distribution of charge, with most charged groups originating from the unevenly distributed LPS molecules (60).

The presence of local surface charge heterogeneity on the cell surface is a significant factor controlling adhesion. Such heterogeneities result in reduction of the electrostatic energy barrier and subsequent deposition of some cells in the primary minimum, despite DLVO predictions that suggest insurmountable barrier for deposition when considering macroscopic cell properties, such as  $\zeta$ -potential (36, 61). Given that the RSPF system only enumerates cells that are irreversibly deposited in a primary energy minimum, the impact of local charge heterogeneity is quite substantial for this system (28). For the packed-bed system, deposition in secondary minima is the dominating mechanism (23), which is affected to a lesser extent by the degree of charge heterogeneity. This is attributed to secondary energy minima existing at greater separation distances than the primary minima—on the order of a few tens of nanometers from the collector surface—where the influence of local charge heterogeneity on the electrostatic double layer interaction is much less pronounced (61). Our experimental results support these proposed mechanisms as the deposition kinetics of the more heterogeneous stationary-phase cells was 10-fold greater than mid-exponential phase cells in the RSPF system, yet only differed up to a factor of 4 in the packed-bed system. Additionally, at higher ionic strength conditions when no electrostatic energy barrier to deposition exists, the deposition rates of mid-exponential and stationary-phase cells were comparable.

## Acknowledgments

This work was supported by funding from the National Science Foundation Collaborative Research Activities in Environmental Molecular Sciences (Grant CHE-0089156) and the National Water Research Institute. We also acknowledge Professor H. P. Spaink (Leiden University, The Netherlands) for the use of the EGFP plasmid.

## Note Added after ASAP Publication

Axis labels in Figures 1 and 4 were incorrect in the version published ASAP May 27, 2005. The corrected version was published ASAP June 8, 2005.

## Literature Cited

- (1) Gross, M. J.; Logan, B. E. Influence of different chemical treatments on transport of *Alcaligenes paradoxus* in porous-media. *Appl. Environ. Microbiol.* **1995**, *61*, 1750–1756.

- (2) Rittmann, B. E. Back to bacteria: A more natural filtration. *Civil Eng.* **1996**, *66*, 50–52.
- (3) Razatos, A.; Ong, Y. L.; Sharma, M. M.; Georgiou, G. Evaluating the interaction of bacteria with biomaterials using atomic force microscopy. *J. Biomater. Sci.-Polym. Ed.* **1998**, *9*, 1361–1373.
- (4) Mohamed, N.; Teeters, M. A.; Patti, J. M.; Hook, M.; Ross, J. M. Inhibition of *Staphylococcus aureus* adherence to collagen under dynamic conditions. *Infect. Immun.* **1999**, *67*, 589–594.
- (5) Lamba, N. M. K.; Baumgartner, J. N.; Cooper, S. L. The influence of thrombus components in mediating bacterial adhesion to biomaterials. *J. Biomater. Sci.-Polym. Ed.* **2000**, *11*, 1227–1237.
- (6) Espinosa-Urgel, M.; Salido, A.; Ramos, J. L. Genetic analysis of functions involved in adhesion of *Pseudomonas putida* to seeds. *J. Bacteriol.* **2000**, *182*, 2363–2369.
- (7) Okte, E.; Sultan, N.; Dogan, B.; Asikainen, S. Bacterial adhesion of *Actinobacillus actinomycetemcomitans* serotypes to titanium implants: SEM evaluation. A preliminary report. *J. Periodontol.* **1999**, *70*, 1376–1382.
- (8) Bloemberg, G. V.; Otoole, G. A.; Lugtenberg, B. J. J.; Kolter, R. Green fluorescent protein as a marker for *Pseudomonas* spp. *Appl. Environ. Microbiol.* **1997**, *63*, 4543–4551.
- (9) Olofsson, A. C.; Hermansson, M.; Elwing, H. *N*-acetyl-L-cysteine affects growth, extracellular polysaccharide production, and bacterial biofilm formation on solid surfaces. *Appl. Environ. Microbiol.* **2003**, *69*, 4814–4822.
- (10) Gannon, J. T.; Manilal, V. B.; Alexander, M. Relationship between cell-surface properties and transport of bacteria through soil. *Appl. Environ. Microbiol.* **1991**, *57*, 190–193.
- (11) van Loosdrecht, M. C. M.; Lyklema, J.; Norde, W.; Schraa, G.; Zehnder, A. J. B. The role of bacterial-cell wall hydrophobicity in adhesion. *Appl. Environ. Microbiol.* **1987**, *53*, 1893–1897.
- (12) Schafer, A.; Harms, H.; Zehnder, A. J. B. Bacterial accumulation at the air–water interface. *Environ. Sci. Technol.* **1998**, *32*, 3704–3712.
- (13) van Loosdrecht, M. C. M.; Lyklema, J.; Norde, W.; Schraa, G.; Zehnder, A. J. B. Electrophoretic mobility and hydrophobicity as a measure to predict the initial steps of bacterial adhesion. *Appl. Environ. Microbiol.* **1987**, *53*, 1898–1901.
- (14) Vigeant, M. A. S.; Ford, R. M.; Wagner, M.; Tamm, L. K. Reversible and irreversible adhesion of motile *Escherichia coli* cells analyzed by total internal reflection aqueous fluorescence microscopy. *Appl. Environ. Microbiol.* **2002**, *68*, 2794–2801.
- (15) Camesano, T. A.; Logan, B. E. Influence of fluid velocity and cell concentration on the transport of motile and nonmotile bacteria in porous media. *Environ. Sci. Technol.* **1998**, *32*, 1699–1708.
- (16) Gross, M.; Cramton, S. E.; Gotz, F.; Peschel, A. Key role of teichoic acid net charge in *Staphylococcus aureus* colonization of artificial surfaces. *Infect. Immun.* **2001**, *69*, 3423–3426.
- (17) Burks, G. A.; Velegol, S. B.; Paramonova, E.; Lindenmuth, B. E.; Feick, J. D.; Logan, B. E. Macroscopic and nanoscale measurements of the adhesion of bacteria with varying outer layer surface composition. *Langmuir* **2003**, *19*, 2366–2371.
- (18) Smets, B. F.; Grasso, D.; Engwall, M. A.; Machinist, B. J. Surface physicochemical properties of *Pseudomonas fluorescens* and impact on adhesion and transport through porous media. *Colloid Surf., B* **1999**, *14*, 121–139.
- (19) Jucker, B. A.; Zehnder, A. J. B.; Harms, H. Quantification of polymer interactions in bacterial adhesion. *Environ. Sci. Technol.* **1998**, *32*, 2909–2915.
- (20) Iwabuchi, N.; Sunairi, M.; Anzai, H.; Morisaki, H.; Nakajima, M. Relationships among colony morphotypes, cell-surface properties and bacterial adhesion to substrata in *Rhodococcus*. *Colloid Surf., B* **2003**, *30*, 51–60.
- (21) Abu-Lail, N. I.; Camesano, T. A. Role of lipopolysaccharides in the adhesion, retention, and transport of *Escherichia coli* JM109. *Environ. Sci. Technol.* **2003**, *37*, 2173–2183.
- (22) Deflaun, M. F.; Tanzer, A. S.; McAteer, A. L.; Marshall, B.; Levy, S. B. Development of an adhesion assay and characterization of an adhesion-deficient mutant of *Pseudomonas fluorescens*. *Appl. Environ. Microbiol.* **1990**, *56*, 112–119.
- (23) Redman, J. A.; Walker, S. L.; Elimelech, M. Bacterial adhesion and transport in porous media: Role of the secondary energy minimum. *Environ. Sci. Technol.* **2004**, *38*, 1777–1785.
- (24) Bruinsma, G. M.; Rustema-Abbing, M.; van der Mei, H. C.; Busscher, H. J. Effects of cell surface damage on surface properties and adhesion of *Pseudomonas aeruginosa*. *J. Microbiol. Methods* **2001**, *45*, 95–101.
- (25) Gottenbos, B.; van der Mei, H. C.; Busscher, H. J. Initial adhesion and surface growth of *Staphylococcus epidermidis* and *Pseudomonas aeruginosa* on biomedical polymers. *J. Biomed. Mater. Res.* **2000**, *50*, 208–214.
- (26) Poortinga, A. T.; Bos, R.; Busscher, H. J. Electrostatic interactions in the adhesion of an ion-penetrable and ion-impenetrable bacterial strain to glass. *Colloid Surf., B* **2001**, *20*, 105–117.
- (27) Yang, J. L.; Bos, R.; Poortinga, A.; Wit, P. J.; Belder, G. F.; Busscher, H. J. Comparison of particle deposition in a parallel plate and a stagnation point flow chamber. *Langmuir* **1999**, *15*, 4671–4677.
- (28) Walker, S. L.; Redman, J. A.; Elimelech, M. Role of cell surface lipopolysaccharides in *Escherichia coli* K12 adhesion and transport. *Langmuir* **2004**, *20*, 7736–7746.
- (29) Huisman, G. W.; Siegele, D. A.; Zambrano, M. M.; Kolter, R. In *Escherichia coli and Salmonella: Cellular and Molecular Biology*, 2nd ed.; Neidhardt, F. C., Ed.; ASM Press: Washington, DC, 1996.
- (30) Manas, P.; Mackey, B. M. Morphological and physiological changes induced by high hydrostatic pressure in exponential- and stationary-phase cells of *Escherichia coli*: Relationship with cell death. *Appl. Environ. Microbiol.* **2004**, *70*, 1545–1554.
- (31) Gmeiner, J.; Schlecht, S. Molecular composition of the outer-membrane of *Escherichia coli* and the importance of protein–lipopolysaccharide interactions. *Arch. Microbiol.* **1980**, *127*, 81–86.
- (32) Ivanov, A. Y.; Fomchenkov, V. M. Dependence of surfactant damage to *Escherichia coli* cells on culture-growth phase. *Microbiology* **1989**, *58*, 785–791.
- (33) Nikaido, H. Molecular basis of bacterial outer membrane permeability revisited. *Microbiol. Mol. Biol. Rev.* **2003**, *67*, 593–656.
- (34) Nikaido, H. In *Escherichia coli and Salmonella: Cellular and Molecular Biology*, 2nd ed.; Neidhardt, F. C., Ed.; ASM Press: Washington, DC, 1996.
- (35) Bonet, R.; Simonpujol, M. D.; Congregado, F. Effects of nutrients on exopolysaccharide production and surface-properties of *Aeromonas salmonicida*. *Appl. Environ. Microbiol.* **1993**, *59*, 2437–2441.
- (36) Song, L. F.; Johnson, P. R.; Elimelech, M. Kinetics of colloid deposition onto heterogeneously charged surfaces in porous-media. *Environ. Sci. Technol.* **1994**, *28*, 1164–1171.
- (37) Elimelech, M.; Nagai, M.; Ko, C. H.; Ryan, J. N. Relative insignificance of mineral grain zeta potential to colloid transport in geochemically heterogeneous porous media. *Environ. Sci. Technol.* **2000**, *34*, 2143–2148.
- (38) Litton, G. M.; Olson, T. M. Colloid deposition kinetics with surface-active agents: Evidence for discrete surface charge effects. *J. Colloid Interface Sci.* **1994**, *165*, 522–525.
- (39) Kihira, H.; Matijevic, E. Kinetics of heterocoagulation. 3. Analysis of effects causing the discrepancy between the theory and experiment. *Langmuir* **1992**, *8*, 2855–2862.
- (40) Feick, J. D.; Velegol, D. Electrophoresis of spheroidal particles having a random distribution of zeta potential. *Langmuir* **2000**, *16*, 10315–10321.
- (41) Feick, J. D.; Velegol, D. Measurements of charge nonuniformity on polystyrene latex particles. *Langmuir* **2002**, *18*, 3454–3458.
- (42) Coughlin, R. T.; Tonsager, S.; McGroarty, E. J. Quantitation of metal-cations bound to membranes and extracted lipopolysaccharide of *Escherichia coli*. *Biochemistry* **1983**, *22*, 2002–2007.
- (43) Jones, J. F.; Feick, J. D.; Imoudu, D.; Chukwumah, N.; Vigeant, M.; Velegol, D. Oriented adhesion of *Escherichia coli* to polystyrene particles. *Appl. Environ. Microbiol.* **2003**, *69*, 6515–6519.
- (44) Razatos, A.; Ong, Y. L.; Sharma, M. M.; Georgiou, G. Molecular determinants of bacterial adhesion monitored by atomic force microscopy. *Proc. Natl. Acad. Sci. U.S.A.* **1998**, *95*, 11059–11064.
- (45) Stuurman, N.; Bras, C. P.; Schlaman, H. R. M.; Wijffes, A. H. M.; Bloemberg, G.; Spaink, H. P. Use of green fluorescent protein color variants expressed on stable broad-host-range vectors to visualize rhizobia interacting with plants. *Mol. Plant–Microbe Interact.* **2000**, *13*, 1163–1169.
- (46) Sambrook, J.; Fritsch, E. F.; Maniatis, T. *Molecular Cloning, A Laboratory Manual*, 2nd ed.; Cold Spring Harbor Laboratory Press: Cold Spring Harbor, NY, 1989; Vol. 3.
- (47) Pembrey, R. S.; Marshall, K. C.; Schneider, R. P. Cell surface analysis techniques: What do cell preparation protocols do to cell surface properties? *Appl. Environ. Microbiol.* **1999**, *65*, 2877–2894.
- (48) Ottewill, R. H.; Shaw, J. N. Electrophoretic studies on polystyrene latices. *J. Electroanal. Chem.* **1972**, *37*, 133.
- (49) Shim, Y.; Lee, H. J.; Lee, S.; Moon, S. H.; Cho, J. Effects of natural organic matter and ionic species on membrane surface charge. *Environ. Sci. Technol.* **2002**, *36*, 3864–3871.

- (50) Kretzschmar, R.; Borkovec, M.; Grolimund, D.; Elimelech, M. Mobile subsurface colloids and their role in contaminant transport. *Adv. Agron.* **1999**, *66*, 121–193.
- (51) Elimelech, M., Gregory, J., Jia, X., Williams, R. A. *Particle Deposition and Aggregation-Measurement, Modeling and Simulation*; Butterworth-Heinemann: New York, 1995.
- (52) Derjaguin, B. V.; Landau, L. *Acta Physicochim. U.S.S.R.* **1941**, *14*, 300.
- (53) Hengge-Aronis, R. In *Escherichia coli and Salmonella: Cellular and Molecular Biology*, 2nd ed.; Neidhardt, F. C., Ed.; ASM Press: Washington, DC, 1996.
- (54) Frank, B. P.; Belfort, G. Polysaccharides and sticky membrane surfaces: critical ionic effects. *J. Membr. Sci.* **2003**, *212*, 205–212.
- (55) Tsuneda, S.; Aikawa, H.; Hayashi, H.; Yuasa, A.; Hirata, A. Extracellular polymeric substances responsible for bacterial adhesion onto solid surface. *FEMS Microbiol. Lett.* **2003**, *223*, 287–292.
- (56) Omoike, A.; Chorover, J. Spectroscopic study of extracellular polymeric substances from *Bacillus subtilis*: Aqueous chemistry and adsorption effects. *Biomacromolecules* **2004**, *5*, 1219–1230.
- (57) Jana, T. K.; Srivastava, A. K.; Csery, K.; Arora, D. K. Influence of growth and environmental conditions on cell surface hydrophobicity of *Pseudomonas fluorescens* in non-specific adhesion. *Can. J. Microbiol.* **2000**, *46*, 28–37.
- (58) Chavant, P.; Martinie, B.; Meylheuc, T.; Bellon-Fontaine, M. N.; Hebraud, M. *Listeria monocytogenes* LO28: Surface physicochemical properties and ability to form biofilms at different temperatures and growth phases. *Appl. Environ. Microbiol.* **2002**, *68*, 728–737.
- (59) Rijnaarts, H. H. M.; Norde, W.; Lyklema, J.; Zehnder, A. J. B. The isoelectric point of bacteria as an indicator for the presence of cell-surface polymers that inhibit adhesion. *Colloid Surf., B* **1995**, *4*, 191–197.
- (60) Kotra, L. P.; Golemi, D.; Amro, N. A.; Liu, G. Y.; Mobashery, S. Dynamics of the lipopolysaccharide assembly on the surface of *Escherichia coli*. *J. Am. Chem. Soc.* **1999**, *121*, 8707–8711.
- (61) Behrens, S. H.; Borkovec, M.; Schurtenberger, P. Aggregation in charge-stabilized colloidal suspensions revisited. *Langmuir* **1998**, *14*, 1951–1954.

Received for review January 14, 2005. Revised manuscript received April 25, 2005. Accepted April 26, 2005.

ES050077T